Proton image and momentum distributions from light-front dynamics

Emanuel Ydrefors

Instituto Tecnológico de Aeronáutica (ITA), Brazil and
Institute of Modern Physics, China

Collaborators: T. Frederico and V. A. Karmanov

Reference: arXiv:2108.02146 [hep-ph]

Perceiving the Emergence of Hadron Mass through AMBER@CERN
(Online)
Sep 29, 2021

Introduction

- In hadron physics, one of the most important remaining challenges is to describe the dynamics and structure of the proton in terms of its basic constituents (quarks and gluons).

- The proton light-front wave function, defined on the null plane $x^+ = t + z = 0$, gives through the parton probability densities access to various observables.

- For example:
    - Electromagnetic form factors
    - The parton distribution function
    - Generalized parton distribution functions

- Additionally, the double parton scattering cross section depends on the double parton distribution function (DPDF) [1]:

$$D(x_1, x_2, \vec{\eta}_\perp) = \sum_{n=3}^{\infty} D_n(x_1, x_2, \vec{q}_\perp) = \sum_{n=3}^{\infty} \int \frac{d^2 k_{1\perp}}{(2\pi)^2} \frac{d^2 k_{2\perp}}{(2\pi)^2} \left\{ \prod_{i \neq 1,2} \int \frac{d^2 k_{i\perp}}{(2\pi)^2} \int_0^1 dx_i \right\}$$
$$\times \delta \left(1 - \sum_{i=1}^{n} x_i \right) \delta \left(\sum_{i=1}^{n} \vec{k}_{i\perp} \right) \Psi_n^\dagger(x_1, \vec{k}_{1\perp} + \vec{\eta}_\perp, x_2, \vec{k}_{2\perp} - \vec{\eta}_\perp, ...) \Psi_n(x_1, \vec{k}_{1\perp}, x_2, \vec{k}_{2\perp}, ...), \tag{1}$$

- The first of Mellin moments of DPDF has recently been calculated within lattice QCD [2].

[1] B. Blok et al, PRD 83 (2011) 071501 (R).

[2] G. S. Bali, JHEP09 (2021) 106.

Motivation: Why another model of the proton?

- The LF wave function is defined on the LF plane, i.e. solely in Minkowski space. In that sense it is not directly available in Euclidean space.
- One alternatice approach is based on Light-front Hamiltonian, e.g. BLFQ (talk by Xingbo Zhao). However, it is usually to limited to a few Fock sectors.
- This motivated us to develop a dynamical three-body model directly in Minkowski space, allowing to compute observables on the LF, ultimately including the full BS amplitude.
- As a first step, Fock basis truncated to valence order and spin degree-of-freedom not included.
- The quark-quark transition amplitude has a pole representing the s-wave diquark introduced through the zero-range interaction between two of the quarks. In that sense it is an effective low-energy model.
- The proton structure will be explored through the LF wave function and its Ioffe-time representation. Results for the momentum distributions will also be presented.

Three-body model
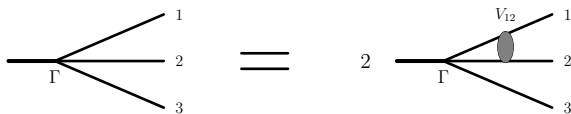
- Three spinless particles of mass *m*. Spectator + pair of interacting particles. Factor of two due to symmetry of wave function with respect to exchange of the particles.
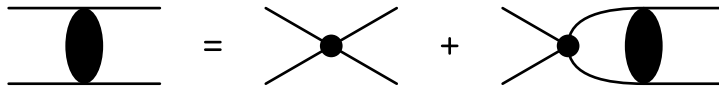
- In the present work a zero-range interaction with four-leg-vertex $i\lambda$ used. Then, for the two-body amplitude (see figure)

$$i\mathcal{F}(M_{12}^2)) = i\lambda + (i\lambda)^2\mathcal{B} + (i\lambda)^3\mathcal{B}^2 + ... = \frac{1}{(i\lambda)^{-1} - \mathcal{B}(M_{12}^2)} \tag{2}$$

with

$$\mathcal{B}(M_{12}^2) = \int \frac{d^4k}{(2\pi)^4} \frac{i}{(k^2 - m^2 + i\epsilon)} \frac{i}{[(k-P)^2 - m^2 + i\epsilon]} \tag{3}$$

- Regularized and renormalized by fixing a diquark pole in the scattering amplitude.

Three-body Faddeev-Bethe-Salpeter equation with zero interaction

- Faddeev-Bethe-Salpeter (FBS) equation with zero interaction [1]:

$$v(q,p) = 2i\mathcal{F}(M_{12}^2) \int \frac{d^4k}{(2\pi)^4} \frac{i}{k^2 - m^2 + i\epsilon} \frac{i}{(p-q-k)^2 - m^2 + i\epsilon} v(k,p) \tag{4}$$

- Currently, bare propagators for the quarks.
- $v(q,p)$ is one of the Faddeev components of the total vertex function.
- Di-quark concept introduced via assuming a pole in $\mathcal{F}(M_{12}^2)$, corresponding either to a two-body bound ($a > 0$) or scattering ($a < 0$) state, where a denotes the scattering length
- $\mathcal{F}(M_{12}^2)$, where $M_{12}^2 = (p-q)^2$, given by

$$\mathcal{F}(M_{12}^2) = \frac{\Theta(-M_{12}^2)}{\frac{1}{16\pi^2 y}\log\frac{1+y}{1-y} - \frac{1}{16\pi ma}} + \frac{\Theta(M_{12}^2)\,\Theta(4m^2 - M_{12}^2)}{\frac{1}{8\pi^2 y'}\arctan y' - \frac{1}{16\pi ma}} + \frac{\Theta(M_{12}^2 - 4m^2)}{\frac{y''}{16\pi^2}\log\frac{1+y''}{1-y''} - \frac{1}{16\pi ma} - \frac{iy''}{16\pi}}, \tag{5}$$

- The FBS equation was recently solved including the infinite number of Fock components in Euclidean [2] and Minkowski [3] space.

[1] T. Frederico, PLB 282 (1992) 409

[2] E. Ydrefors et al, PLB 770 (2017) 131

[3] E. Ydrefors et al, PLB 791 (2019) 276

Valence LF equation

- After the LF projection, i.e. introducing $k_\pm = k_0 \pm k_z$ and integrating over k_-, one obtains the three-body LF equation [1, 2]:

$$\Gamma(x, k_\perp) = \frac{\mathcal{F}(M_{12}^2)}{(2\pi)^3} \int_0^{1-x} \frac{dx'}{x'(1-x-x')} \int_0^\infty \frac{d^2 k'_\perp}{M_0^2 - M_N^2} \Gamma(x', k'_\perp) \quad (6)$$

with the squared free three-body mass

$$M_0^2 = (k'^2_\perp + m^2)/x' + (k_\perp^2 + m^2)/x + ((k'_\perp + k_\perp)^2 + m^2)/(1-x-x') \quad (7)$$

- The three-body valence LF wave function is given by

$$\Psi_3(x_1, \vec{k}_{1\perp}, x_2, \vec{k}_{2\perp}, x_3, \vec{k}_{3\perp}) = \frac{\Gamma(x_1, \vec{k}_{1\perp}) + \Gamma(x_2, \vec{k}_{2\perp}) + \Gamma(x_3, \vec{k}_{3\perp})}{\sqrt{x_1 x_2 x_3}(M_N^2 - M_0^2(x_1, \vec{k}_{1\perp}, x_2, \vec{k}_{2\perp}, x_3, \vec{k}_{3\perp}))}, \quad (8)$$
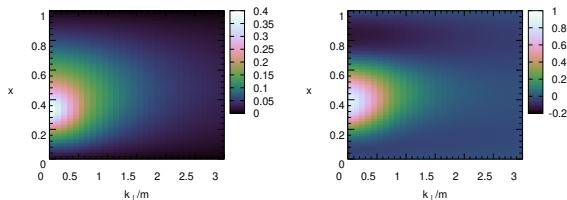
where due to momentum conservation: $x_3 = 1 - x_2 - x_3$ and $\vec{k}_{3\perp} = -\vec{k}_{1\perp} - \vec{k}_{2\perp}$.

[1] J. Carbonell and V.A. Karmanov, PRC 67 (2003) 037001

[2] T. Frederico, PLB 282 (1992) 409

Results for the vertex function

Model	m [MeV]	a $[m^{-1}]$	M_2 [MeV]	M_N/m	r_{F_1} [fm]
I	317	-1.84	-	2.97	0.97
II	362	3.60	681	2.60	0.72

- Two different values of a considered, with negative and positive a, fitted to reproduce the experimental Dirac form factor (up to $\sim 1\,\mathrm{GeV}^2$). For the model with a bound diquark the obtained value of the di-quark mass same as a recent Lattice QCD calculation.
- The proton structure contained in the vertex function $\Gamma(x, k_\perp)$. As seen for the bound diquark case it has a node at roughly $x = 0.8$.
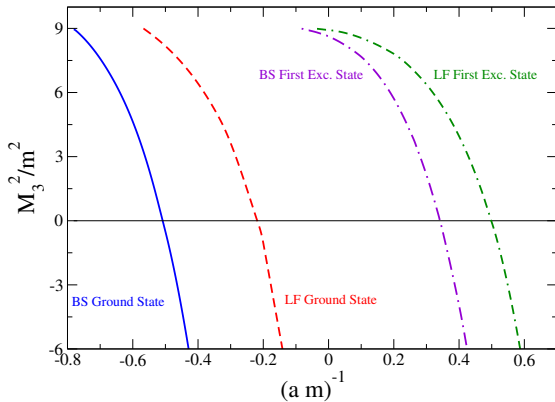
- As studied in PLB 770 (2017) 131, it exists a lower-lying unphysical solution with $M_N^2 < 0$. This is the relativistic analog of the well-known Thomas collapse. But, contrary to the non-relativistic case the unphysical state has a finite energy, due to a short-range repulsion of purely relativistic origin.
- Difference between valence LF result and full BS solution, due to a contribution coming from an infinite number of diagrams involving anti-particles, which can be interpreted as an effective three-body force.
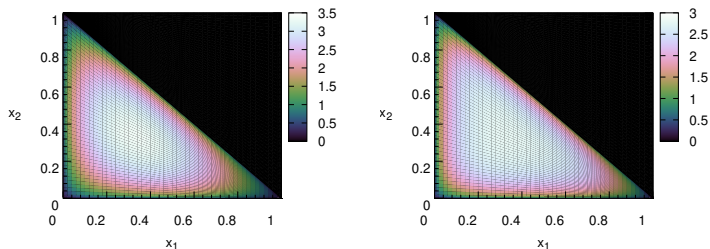
- The distribution amplitude is defined as

$$\phi(x_1, x_2) = \int d^2 k_{1\perp} d^2 k_{2\perp} \Psi_3(x_1, \vec{k}_{1\perp}, x_2, \vec{k}_{2\perp}, x_3, \vec{k}_{3\perp}). \tag{9}$$

- It shows the dependence of the wave function on the momentum fractions for the case when the quarks share the same position.
- For the two considered cases similar results.

Ioffe-time image of the valence state

- Alternatively, the proton can be studied in the on the null-plane, in terms of the transverse position ($\vec{b}_{i\perp}$) and the Ioffe-time $\tilde{x}_i = b_i^- p^+$. The image of the proton is then obtained through the Fourier transform of the proton LF wave function.

- For simplicity, we consider here the case $\vec{b}_{1\perp} = \vec{b}_{2\perp} = \vec{0}_\perp$, and then one has

$$\Phi(\tilde{x}_1, \tilde{x}_2) \equiv \tilde{\Psi}_3(\tilde{x}_1, \vec{0}_\perp, \tilde{x}_2, \vec{0}_\perp) = \int_0^1 dx_1 \, e^{i\tilde{x}_1 x_1} \int_0^{1-x_1} dx_2 \, e^{i\tilde{x}_2 x_2} \, \phi(x_1, x_2) \,, \qquad (10)$$
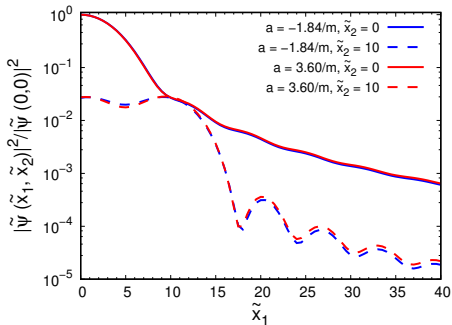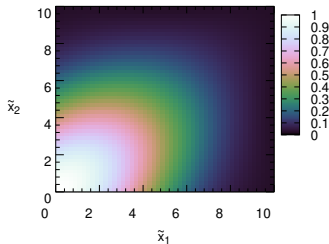
- For $\tilde{x}_2 = 0$ the two parameter sets give almost identical results.
- For $\tilde{x}_2 = 10$ and $\tilde{x}_1 >= 10$ a rather dramatic decrease of the amplitude is seen. Similar behavior for the two parameter sets.
- An exponential damping is seen with respect to the relative distance in Ioffe-time between the two quarks. We expect this damping to be even more significant if confinement is incorporated, as its more effective at large distances.

Electromagnetic form factor

- The valence contribution to the Dirac form factor is given by

$$F_1(Q^2) = \left\{ \prod_{i=1}^{3} \int \frac{d^2 k_{i\perp}}{(2\pi)^2} \int_0^1 dx_i \right\} \delta \left(1 - \sum_{i=1}^{3} x_i \right) \delta \left(\sum_{i=1}^{3} \vec{k}_{i\perp}^{\text{f}} \right)$$
$$\times \Psi_3^\dagger(x_1, \vec{k}_{1\perp}^{\text{f}}, ...) \Psi_3(x_1, \vec{k}_{1\perp}^{\text{i}}, ...), \tag{11}$$
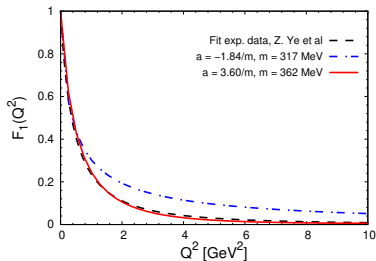
where $Q^2 = \vec{q}_\perp \cdot \vec{q}_\perp$ and the magnitudes of the momenta read

$$\left| \vec{k}_{i\perp}^{\text{f(i)}} \right|^2 = \left| \vec{k}_{i\perp} \pm \frac{\vec{q}_\perp}{2} x_i \right|^2 = \vec{k}_{i\perp}^2 + \frac{Q^2}{4} x_i^2 \pm \vec{k}_{i\perp} \cdot \vec{q}_\perp x_i \quad (i = 1, 2), \tag{12}$$
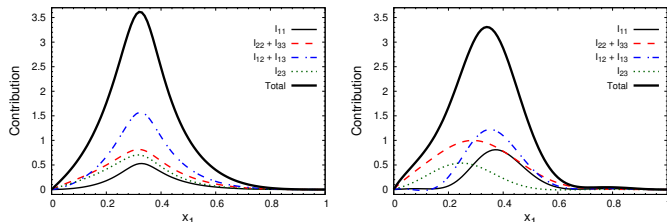
and

$$\left| \vec{k}_{3\perp}^{\text{f(i)}} \right|^2 = \left| \pm \frac{\vec{q}_\perp}{2}(x_3 - 1) - \vec{k}_{1\perp} - \vec{k}_{2\perp} \right|^2 =$$
$$(1 - x_3)^2 \frac{Q^2}{4} \pm (1 - x_3) \vec{q}_\perp \cdot (\vec{k}_{1\perp} + \vec{k}_{2\perp}) + (\vec{k}_{1\perp} + \vec{k}_{2\perp})^2. \tag{13}$$

- Both parameters give a fair reproduction of experimental data for low Q^2, i.e $Q^2 < 1\text{GeV}^2$, where the model should be applicable.
- The diquark case give also quite good agreement for moderate Q^2. But, this should be viewed with caution since the scaling laws of the QCD are not built-in.

- We define the single parton distribution function (PDF) as

$$f_1(x_1) = \frac{1}{(2\pi)^6} \int_0^{1-x_1} dx_2 \int d^2 k_{1\perp} d^2 k_{2\perp} |\Psi_3(x_1, \vec{k}_{1\perp}, x_2, \vec{k}_{2\perp}, x_3, \vec{k}_{3\perp})|^2 = \tag{14}$$
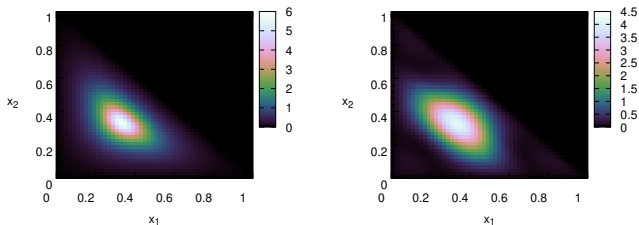
$$I_{11} + I_{22} + I_{33} + I_{12} + I_{13} + I_{23}.$$

with the Faddeev contributions

$$I_{ii} = \frac{1}{(2\pi)^6} \int_0^{1-x_1} dx_2 \int d^2 k_{1\perp} d^2 k_{2\perp} \frac{\Gamma^2(x_i, \vec{k}_{i\perp})}{x_1 x_2 x_3 (M_N^2 - M_0^2(x_1, \vec{k}_{1\perp}, x_2, \vec{k}_{2\perp}, x_3, \vec{k}_{3\perp}))^2}$$

$$I_{ij} = \frac{2}{(2\pi)^6} \int_0^{1-x_1} dx_2 \int d^2 k_{1\perp} d^2 k_{2\perp} \frac{\Gamma(x_i, \vec{k}_{i\perp})\Gamma(x_j, \vec{k}_{j\perp})}{x_1 x_2 x_3 (M_N^2 - M_0^2(x_1, \vec{k}_{1\perp}, x_2, \vec{k}_{2\perp}, x_3, \vec{k}_{3\perp}))^2}; \quad i \neq j. \tag{15}$$

- Evolution of the PDF will be performed in the near future.

- The valence double parton distribution function (DPDF) is given by

$$
\begin{aligned}
D_3(x_1, x_2; \vec{\eta}_\perp) = \frac{1}{(2\pi)^6} \int d^2 k_{1\perp} d^2 k_{2\perp} \\
\times \Psi_3^\dagger(x_1, \vec{k}_{1\perp} + \vec{\eta}_\perp; x_2, \vec{k}_{2\perp} - \vec{\eta}_\perp; x_3, \vec{k}_{3\perp}) \Psi_3(x_1, \vec{k}_{1\perp}; x_2, \vec{k}_{2\perp}; x_3, \vec{k}_{3\perp}).
\end{aligned}
\tag{16}
$$

- Fourier transform of $D_3(x_1, x_2, \vec{\eta}_\perp)$ in $\vec{\eta}_\perp$ gives the probability of finding the quarks 1 and 2 with momentum fractions x_1 and x_2 at a relative distance $\vec{y}_\perp$ within the proton.

- In the figure is shown results for $\eta_\perp = 0$. For the case of virtual diquark (left panel) a rather narrow distribution is obtained due to the small binding energy.
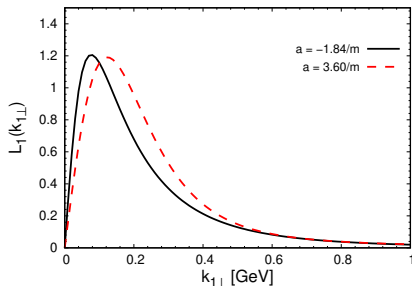
- The single quark transverse momentum density in the forward limit and integrated in the longitudinal momentum is associated with the probability density to find a quark with momentum $k_\perp$.
- It can be computed as:

$$L_1(k_{1\perp}) = \frac{k_{1\perp}}{(2\pi)^6} \int_0^1 dx_1 \int_0^{1-x_1} dx_2 \int_0^{2\pi} d\theta_1 \int d^2k_{2\perp} |\psi_3(x_1, \vec{k}_{1\perp}, x_2, \vec{k}_{2\perp}, x_3, \vec{k}_{3\perp})|^2.$$

(17)

- For model I (solid line) a more narrow distribution is seen compared to model II (dashed line), because the radius is larger.
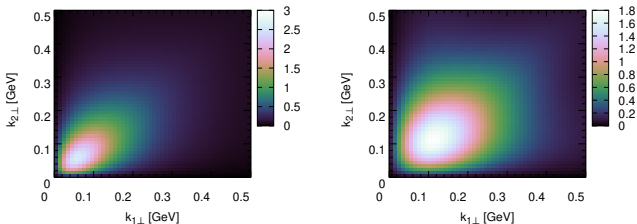
- The corresponding two-quark one reads

$$
L_2(k_{1\perp}, k_{2\perp}) = \frac{k_{1\perp} k_{2\perp}}{(2\pi)^6} \int_0^1 dx_1 \int_0^{1-x_1} dx_2 \int_0^{2\pi} d\theta_1 \int_0^{2\pi} d\theta_2 \\
\times |\psi_3(x_1, \vec{k}_{1\perp}, x_2, \vec{k}_{2\perp}, x_3, \vec{k}_{3\perp})|^2.
$$
(18)

- The more compact configuration of model II is reflected in the wider distribution, and the probability density peak is consistent with the results for the one-quark distribution.
- L_1 and L_2 only depend on transverse variabels, and should thus be the same in Minkowski and Euclidean spaces. It thus makes a comparison with approaches such as Lattice QCD or DSE feasible.

Work in progress: Going beyond the valence order

- The three-body FBS equation with zero-range interaction, including the infinite number of Fock components, was solved by direct integration in Minkowski space in Ref. [1]. However, the solution was quite difficult from numerical point of view.

- However, like in the two-body case, the Nakanishi integral representation be used for vertex function:

$$v(q;p) = \int_{-4/3}^{2/3} dz \int_0^\infty \frac{d\gamma\, g(\gamma,z)}{\gamma - k^2 - (p \cdot q)z - i\epsilon} \tag{19}$$

- For the two-body scattering amplitude

$$\mathcal{F}(M_{12}^2) = \int_{4m^2}^\infty d\gamma \frac{\rho(\gamma)}{M_{12}^2 - \gamma + i\epsilon} \tag{20}$$

with the spectral function

$$\rho(\gamma) = -\frac{\theta(s - 4m^2)}{16\pi^2} \frac{y''}{\left(\frac{y''}{16\pi^2} \log \frac{1+y''}{1-y''} - \frac{1}{16\pi ma}\right)^2 + \left(\frac{y''}{16\pi}\right)^2} \tag{21}$$

- Construction of the integral equation for $g(\gamma,z)$ and its solution is under development.

[1] E. Ydrefors et al, PLB 791 (2019) 276

Conclusions

- We have, in this work, studied the proton in a simple but fully dynamical valence LF model based on a zero-range interaction.
- The model is based on the concept of a strongly interacting diquark, either virtual or bound.
- We have studied the structure of the proton by computing the LF wave function in its Ioffe-time representation and also momentum distributions.
- However, the model is rather crude since e.g. the spin degree of freedom hasn't been included yet. But is a first step towards studying the proton directly in Minkowski space.
- Future plans:
  - Generalization to the infinite set of Fock components (The Faddeev-Bethe-Salpeter equation solved in PLB 791 (2019) 276)
  - Implementation of a more realistic interaction (gluon exchange)
  - Inclusion of spin degree of freedom